JACS
JOURNAL OF THE AMERICAN CHEMICAL SOCIETY
Article
pubs.acs.org/JACS

Li–O_2 Battery with a Dimethylformamide Electrolyte

Yuhui Chen,[†] Stefan A. Freunberger,[†] Zhangquan Peng,[†] Fanny Bardé,[‡] and Peter G. Bruce*[,†]

[†]School of Chemistry, University of St. Andrews, North Haugh, St. Andrews, Fife KY16 9ST, United Kingdom
[‡]Toyota Motor Europe, Technical Centre, Hoge Wei 33 B, B-1930 Zaventem, Belgium

Supporting Information

ABSTRACT: Stability of the electrolyte toward reduced oxygen species generated at the cathode is a crucial challenge for the rechargeable nonaqueous Li–O_2 battery. Here, we investigate dimethylformamide as the basis of an electrolyte. Although reactions at the O_2 cathode on the first discharge–charge cycle are dominated by reversible Li_2O_2 formation/decomposition, there is also electrolyte decomposition, which increases on cycling. The products of decomposition at the cathode on discharge are Li_2O_2, Li_2CO_3, HCO_2Li, CH_3CO_2Li, NO, H_2O, and CO_2. Li_2CO_3 accumulates in the electrode with cycling. The stability of dimethylformamide toward reduced oxygen species is insufficient for its use in the rechargeable nonaqueous Li–O_2 battery.

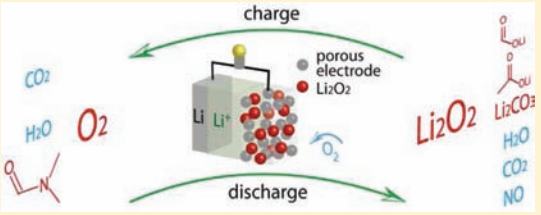

INTRODUCTION

The long-term need for a step change in energy storage coupled with the high theoretical specific energy of the Li–O_2 battery has led to intense interest in such batteries, based on aqueous and nonaqueous electrolytes.[1−27] While many problems face their practical realization, the electrolyte presents a particular challenge.[28−30] In the case of the nonaqueous Li–O_2 battery, the reaction at the cathode involves, on discharge, O_2 being reduced to O_2^{2-}, which when combined with Li^+ leads to the final discharge product Li_2O_2. Charging involves oxidation of Li_2O_2 back to Li^+ and O_2.[3,10,14,15,18,31−39] A suitable nonaqueous electrolyte for a Li–O_2 cell must support formation of Li_2O_2 at the cathode in high purity on discharge and its reversible decomposition on charge, with this process being sustained on cycling. Early work on nonaqueous electrolytes for Li–O_2 cells focused on organic carbonates (e.g., propylene carbonate), but these are susceptible to nucleophilic attack by the reduced O_2 species at the cathode.[31,32,39−41] Significant attention has been given to ethers (e.g., tetraglyme or dimethoxyethane); although, as expected, they proved more stable than the organic carbonates, they still exhibit decomposition on cycling.[31,33,42] Exploring alternative electrolytes is a timely priority.[29,43,44]

Here, we investigate dimethylformamide (DMF) as the basis of an electrolyte for the Li–O_2 battery. DMF was chosen because it has been used as a solvent for O_2 reduction in the presence of molecular cations, such as TBA^+, and the reduced oxygen species, O_2^-, is reported to be stable.[35,45,46] In contrast, here we show that in the presence of Li^+, although DMF is more stable toward reduced oxygen than organic carbonates and is capable of forming Li_2O_2 at the cathode in relatively high purity on the first discharge, with its complete removal on subsequent charge, results reveal that the degree of side reaction increases on cycling with accumulation of Li_2CO_3, HCO_2Li, and CH_3CO_2Li in the cathode, Scheme 1. On the basis of their instability at the cathode alone, DMF electrolytes are not suitable for Li–O_2 batteries. We also show extension of this work to related amides, dimethylacetamide (DMA) and *N*-methyl-2-pyrrolidone (NMP), which demonstrate that the instability is not confined to DMF.

Scheme 1. Proposed Mechanism for Reactions Occurring during Discharge

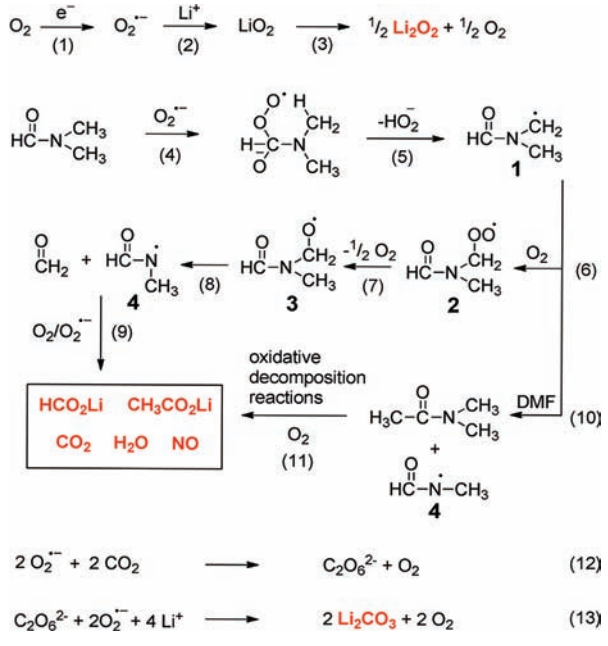

RESULTS AND DISCUSSION

Cells containing 0.1 M $LiClO_4$ in DMF as the electrolyte and a composite cathode composed of Super P carbon and PTFE

Received: March 5, 2012
Published: April 19, 2012

   dx.doi.org/10.1021/ja302178w | J. Am. Chem. Soc. 2012, 134, 7952−7957

were constructed as described in the Supporting Information. $LiClO_4$ was chosen as the salt because it can be obtained in high purity and may be rigorously dried.

First Discharge–Charge. The load curve for the first discharge–charge cycle is shown in Figure 1. Discharge occurs

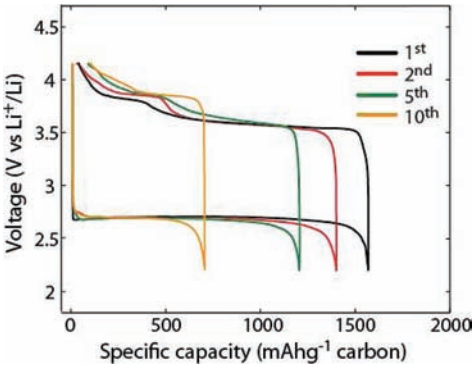

Figure 1. Load curves for a cell containing 0.1 M $LiClO_4$ in DMF and a composite cathode, Super P carbon–PTFE, rate 70 mAg^{-1} (carbon), 50 μAcm^{-2} (geometric).

at ~2.7 V versus Li^+/Li. The charging curve exhibits several features. A small inflection is observed at 3.1–3.5 V, followed by a plateau at ~3.6 V and a second plateau at 3.8–3.9 V.

To investigate the stability of the electrolyte, the products formed at the end of discharge and charge were determined by a combination of FTIR, powder X-ray diffraction (PXRD), differential electrochemical mass spectrometry (DEMS), and NMR. At the end of the first discharge the cathode was removed and examined by PXRD and FTIR, Figures 2 and 3,

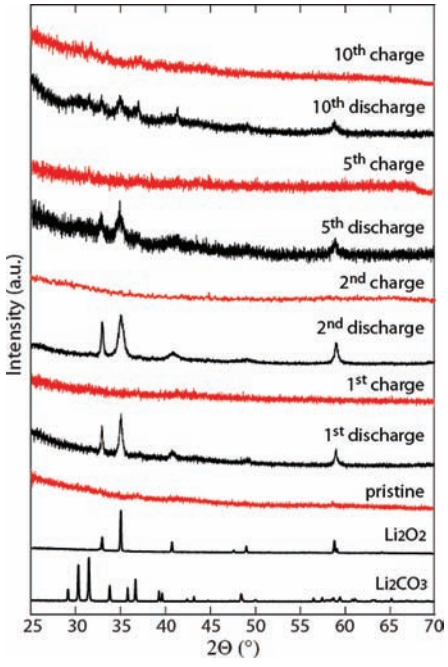

Figure 2. PXRD patterns (Cu Kα) of Super P carbon–PTFE composite electrodes cycled in 0.1 M $LiClO_4$ in DMF, rate 70 mAg^{-1} (carbon). Diffraction patterns in red correspond to the pristine electrode and electrodes at the end of charge after the indicated number of cycles.

respectively. Li_2O_2 was observed along with some evidence of residual DMF in the FTIR spectrum. In order to probe the

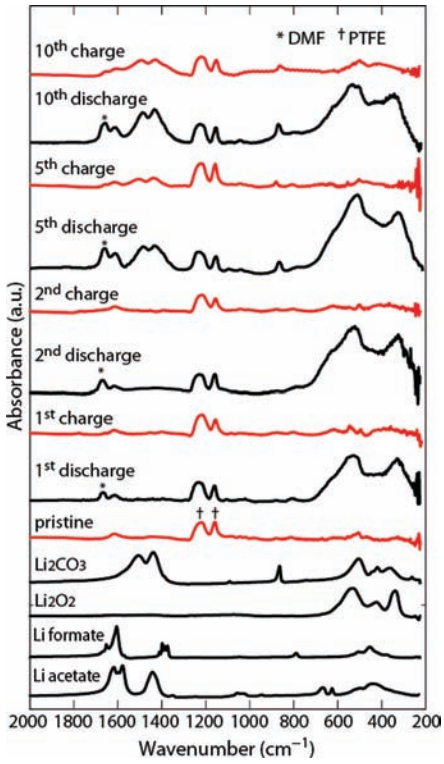

Figure 3. FTIR spectra of Super P carbon–PTFE composite electrodes cycled in 0.1 M $LiClO_4$ in DMF, rate 70 mAg^{-1} (carbon). Spectra in red correspond to the pristine electrode and electrodes at the end of charge after the indicated number of cycles.

reactions on discharge in more detail, in particular, electrolyte stability, in situ DEMS was carried out, Figure 4. O_2 gas was consumed, as expected. The quantity was compared with the charge passed and gave an e^-/O_2 ratio of 1.97 (Table 1), close to the theoretical value of 2 for pure Li_2O_2 formation and in accord with the PXRD and FTIR data. However, evidence of a small degree of DMF degradation is seen in the observation of a very small amount of NO gas (<0.1% of O_2) evolution on discharge, Figure 4a. To identify the products of electrolyte decomposition, a discharged electrode was washed with D_2O and the resulting solution subjected to ^1H NMR. As shown previously, this method permits identification of compounds that may not be assigned from FTIR alone.[32,33]

^1H NMR (Figure S1a, Supporting Information) shows evidence of HCO_2Li and CH_3CO_2Li. We can conclude that the products at the end of the first discharge are overwhelmingly dominated by Li_2O_2 (PXRD and FTIR), but there is also evidence of the beginning of DMF decomposition (DEMS and ^1H NMR).

On charging, all discharge products were removed; none of the peaks associated with Li_2O_2 in the PXRD or FTIR spectra remain, Figures 2 and 3, and ^1H NMR shows no evidence of residual HCO_2Li and CH_3CO_2Li, Figure S1b, Supporting Information. The DEMS data on the first charge showed only O_2 evolution, Figure 4b, and with an e^-/O_2 ratio of 1.96. The lack of any detectable CO_2 and H_2O evolution expected from oxidation of HCO_2Li and CH_3CO_2Li[32,33] confirms that the amount of electrolyte decomposition occurring on the first discharge is very small. The DEMS data on charging reveal the presence of three peaks in the current passed and flux of O_2 evolved with onsets at ~3.1, 3.5, and 3.8 V. These are in accord

dx.doi.org/10.1021/ja302178w | J. Am. Chem. Soc. 2012, 134, 7952–7957

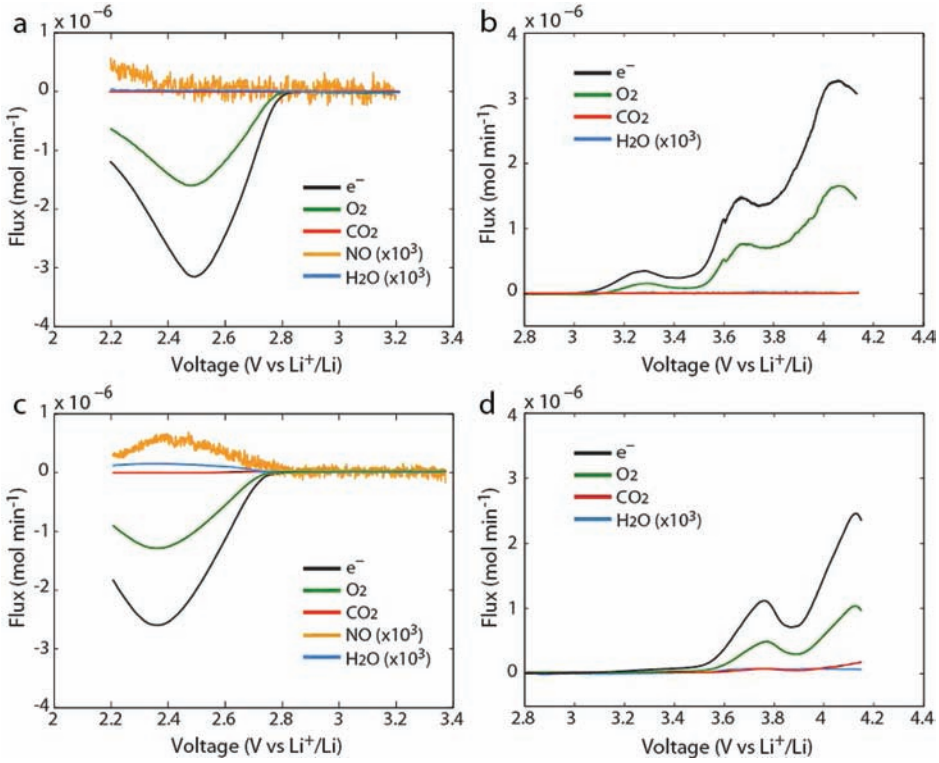

Figure 4. In situ DEMS of a cell containing 0.1 M $LiClO_4$ in DMF and a Super P carbon–PTFE composite electrode: (a) first discharge, (b) first recharge, (c) fifth discharge, and (d) fifth recharge, scan rate 0.05 mVs^{-1}. Note the NO and H_2O fluxes are magnified by 10^3 to make them visible on the same plot. Current decrease during discharge is due to increasing filling of the electrode with product.

Table 1. Ratio of Charge Passed to O_2 Consumed/Evolved on Discharge/Charge for a Cell Containing 0.1M $LiClO_4$ in DMF

	ratio (e^-/O_2)
first discharge[a]	1.97
first charge[a]	1.96
second discharge[a]	2.00
second charge[a]	2.00
first discharge[b]	1.98
first charge[b]	1.96

[a]With Super P carbon–PTFE composite electrode. [b]With nanoporous gold electrode.

with the three features observed in the load curve for the first charge, Figure 1. Such stepwise oxidation of Li_2O_2 has been observed previously by others.[31,44] It has been attributed to heterogeneity in the electrodes leading to oxidation being more facile in certain regions of the electrode than others.[31] The electrolyte at the end of discharge and charge was investigated by NMR spectroscopy, and no peaks from any impurities were detected. Together the PXRD, FTIR, NMR, and DEMS data demonstrate that the first discharge–charge cycle in DMF is dominated by reversible Li_2O_2 formation with a very small degree of electrolyte degradation.

Cycling. In order to examine the effect of cycling on the stability of DMF, a series of discharge–charge cycles was carried out, Figure 1. The charge plateau at ~3.6 V decreases as capacity fades on cycling until at 10 cycles only the higher voltage plateau at 3.9 V remains. The cathode at the end of discharge and charge was examined as a function of cycling by PXRD, FTIR, NMR, and DEMS, Figures 2, 3, 4S1, and S2, Supporting Information. These data reveal that the behavior on the second cycle is similar to the first, i.e., mainly reversible Li_2O_2 formation/decomposition.

However, on the fifth cycle there is clear evidence in the FTIR of significant side reactions at the end of discharge. Peaks in addition to Li_2O_2 can be assigned to Li_2CO_3 and HCO_2Li/CH_3CO_2Li (due to overlap of the bands from HCO_2Li, CH_3CO_2Li, and Li_2CO_3 it is difficult to distinguish the formate from the acetate). ^1H NMR, after washing the discharged electrode with D_2O, confirmed the presence of HCO_2Li and CH_3CO_2Li in the electrode at the end of the fifth discharge, Figure S1e, Supporting Information. Only the most prominent diffraction peaks of Li_2CO_3 can just be observed in the PXRD data at the end of the fifth discharge, Figure 2. This highlights the fact the PXRD alone is insufficient to characterize the products of discharge: Li_2O_2 is observable, but less crystalline compounds cannot be detected.

Although the PXRD data at the end of the fifth charge suggest that all the Li_2O_2 and Li_2CO_3 formed on discharge had been oxidized on charge, Figure 2, FTIR again proves more revealing. Figure 3 shows that at the end of charge after 5 cycles, although Li_2O_2 and much of the decomposition products have indeed been removed on charging, there is evidence that some of the latter remain, principally Li_2CO_3. This is in accord with our previous studies of the oxidation of various organolithium compounds and Li_2CO_3, which showed that compounds such as HCO_2Li and CH_3CO_2Li can be decomposed below 4 V but that although oxidation of Li_2CO_3 is possible it is less facile and often incomplete, even when charged above 4 V.[32] As a result of the sluggish (and hence incomplete) oxidation of Li_2CO_3, it increases in proportion with cycling, see 10th charge in Figure 3. In short, Li_2CO_3 becomes the dominant side product and accumulates in the

dx.doi.org/10.1021/ja302178w | J. Am. Chem. Soc. 2012, 134, 7952–7957

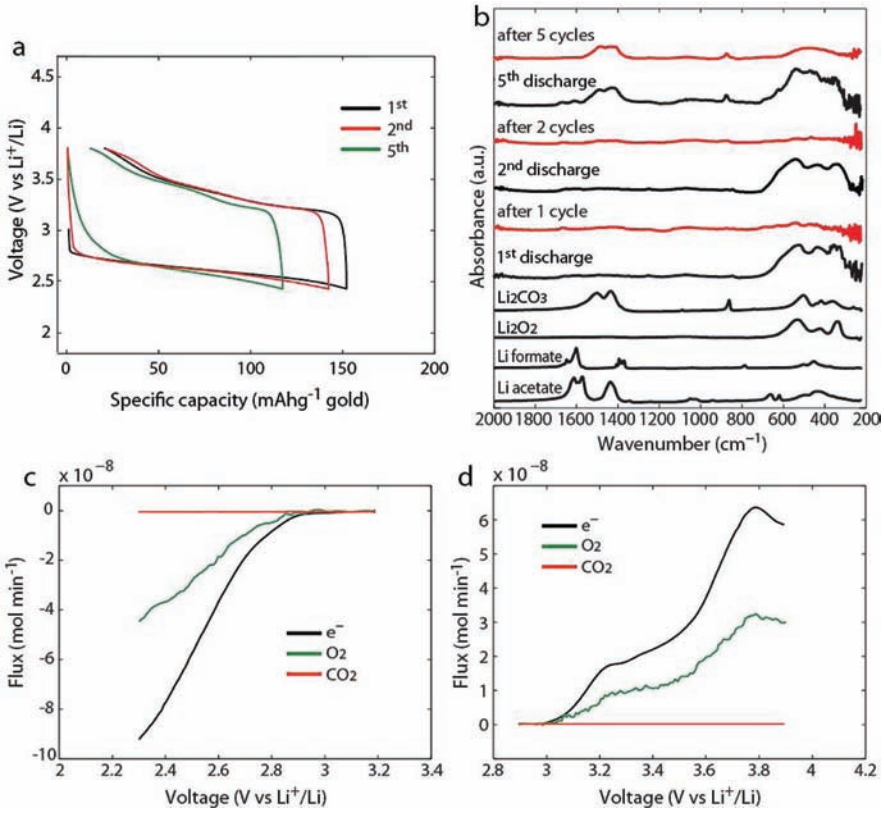

Figure 5. (a) Load curves, (b) FTIR spectra, (c) in situ DEMS on first discharge, and (d) first recharge for a cell containing 0.1 M $LiClO_4$ in DMF and a nanoporous gold cathode: rate = 500 mAg^{-1} (Au), 50 $\mu A\ cm^{-2}$ (geometric).

electrode on cycling, in accord with the capacity fading, Figure 1. We anticipate that as the Li_2CO_3 accumulates in the electrode on cycling it increasingly blocks the electrode surface, resulting in the observed capacity fading.

The increasing electrolyte decomposition on cycling is also evident in the in situ DEMS data, Figure 4. Discharge on cycle 5 is accompanied by evolution of NO and H_2O. On subsequent charging, the peak in the current and O_2 flux observed on the first charge at 3.3 V is barely apparent; however, the peaks at ~3.7 and ~4 V persist, although they are shifted slightly to higher voltages. In contrast to the first charge, there is evidence of CO_2 evolution on the fifth charge, and it occurs at similar potentials to O_2 evolution, Figure 4d. There is also some evidence of H_2O gas evolution. Overall, the DEMS data indicate that on cycling the charging process is still mainly Li_2O_2 oxidation but accompanied by oxidation of the products of electrolyte decomposition.

Salt and Electrode. To verify that the side reactions are due to the DMF solvent and not the salt or electrode the former was replaced with LiTFSI and in a separate experiment the Super P cathode was replaced with nanoporous gold. No significant difference in the nature or extent of the decomposition products upon cycling was observed by replacing $LiClO_4$ with LiTFSI, as expected, Figures S3, S4, and S5, Supporting Information. The load curves using a nanoporous gold electrode are shown in Figure 5, along with the corresponding FTIR data. Charging again exhibits two plateaus, although the overall charging voltage is significantly lower than with Super P. There is currently a debate about the possible role of electrocatalysis in Li_2O_2 oxidation.[10,16] It has been suggested that Au lowers the oxidation potential.[16] There does seem to be an effect of substrate on the charging potential in DMF, but whether this is electrocatalysis or arises for other factors is not yet clear. FTIR data at the end of discharge and charge reveal similar results to those observed for Super P, with the first cycle being dominated by reversible Li_2O_2 formation and evidence of increasing decomposition of electrolyte on cycling. This is confirmed by ^1H NMR, Figure S6, Supporting Information. In situ DEMS data also reveals O_2 is consumed on the first discharge, with an e^-/O_2 ratio of 1.98, and on subsequent charging, evolved with an e^-/O_2 ratio of 1.96, Table 1. Again, in situ DEMS reveals the stepwise oxidation of Li_2O_2 in accord with the charging curves in Figure 5a. Overall, it may be concluded that the increasing presence of side-reaction products as a function of cycling arises from the electrolyte and not from the electrode substrate, since similar results are obtained with two very different substrates, Super P carbon and nanoporous gold.

DMA and NMP. To demonstrate that the instability is not confined to DMF, the related amides DMA and NMP were also investigated. The FTIR data, Figure S7, Supporting Information, show that Li_2O_2 is the dominant product in DMA at the end of the first discharge, and the presence of Li_2O_2 is reinforced by the PXRD data, Figure S8, Supporting Information. The presence of CH_3CO_2Li and HCO_2Li is confirmed by the D_2O ^1H NMR data, Figure S9, Supporting Information. Decomposition is even more severe in the case of NMP, with clear evidence of Li_2CO_3, CH_3CO_2Li, and HCO_2Li in the FTIR, corroborated by D_2O ^1H NMR, and no evidence of Li_2O_2 in the PXRD data.

Mechanism of Electrolyte Decomposition. A mechanism by which the electrolyte decomposes is shown in Scheme 1. Commencing with O_2 reduction to $O_2^{\bullet-}$, reaction 1, $O_2^{\bullet-}$ either can react with Li^+ ions to form LiO_2 and then Li_2O_2,

dx.doi.org/10.1021/ja302178w | J. Am. Chem. Soc. 2012, 134, 7952−7957

reactions 2 and 3,[18] or may attack the CO group of the amide, yielding a tetrahedral intermediate, reaction 4, followed by a 6-membered cyclic transition state to form a carbon radical, reaction 5.[47,48] The resulting carbon-centered radical **1** can react with DMF and O_2.[49] Reaction with an O_2 molecule, reaction 6, leads to the peroxo radical **2**, which proceeds via a dimer[49,50] to the alkoxy radical **3** and further to the intermediate **4** and formaldehyde. Subsequent reaction with O_2/$O_2^{\bullet-}$, reaction 9, results in formation of HCO_2Li, CO_2, H_2O, and NO. Reaction of intermediate **1** with another DMF molecule can form acetamide and intermediate **4**, reaction 10. This can be followed by oxidative decomposition,[47,49,51] reaction 11. Li_2CO_3 can form by reactions 12 and 13, as described previously.[32,52,53] The absence of CO_2 in the DEMS on discharge is likely due to its rapid consumption upon evolution by reactions 12 and 13. It should be noted that the initial attack on the DMF molecule could come from LiO_2 instead of $O_2^{\bullet-}$. Scheme 1 is in accord with detection of the final products, Li_2O_2, Li_2CO_3, HCO_2Li, CH_3CO_2Li, CO_2, H_2O, and NO, by FTIR, PXRD, NMR, and DEMS.

CONCLUSIONS

Reactions occurring at the O_2 cathode in a Li−O_2 cell on cycling in a dimethylformamide-based electrolyte have been investigated with a range of techniques including FTIR, powder X-ray diffraction, ^{1}H solution NMR, and in situ differential electrochemical mass spectrometry. The first discharge−charge cycle is dominated by reversible Li_2O_2 formation/decomposition, associated with a 0.9 V gap between charge and discharge. However, ^{1}H NMR and differential electrochemical mass spectrometry indicate a very minor degree of electrolyte decomposition, even on the first discharge. Decomposition increases on cycling, such that after five cycles there is a significant presence of Li_2CO_3, HCO_2Li, and CH_3CO_2Li in the cathode at the end of discharge. Li_2CO_3 is not completely oxidized on charging, in accord with previous results,[32] and hence, the residual Li_2CO_3 accumulates on cycling, likely increasingly blocking the electrode surface, in accord with the observed capacity fading. A reaction scheme is presented for decomposition of dimethylformamide due to reaction with reduced O_2 species. The stability of dimethylformamide in a Li−O_2 cell is superior to organic carbonates and to a range of linear and cyclic ethers, both of which show a greater degree of electrolyte decomposition on the first discharge. Nevertheless, it may be concluded that the stability of dimethylformamide toward reduced oxygen species is not sufficient for a rechargeable nonaqueous Li−O_2 cell. DMF is also not sufficiently stable toward Li metal for operation in a Li−O_2 cell. However, the Li anode could be protected by a Li^+ conducting ceramic, like LISICON, to mitigate reaction between it and the electrolyte, something that may be required in any case (i.e., regardless of the electrolyte stability) to avoid reaction between the anode and O_2. The search for a stable electrolyte for the Li−O_2 cell remains an important task.

ASSOCIATED CONTENT

Supporting Information

Experimental procedure, ^{1}H solution NMR, in situ DEMS of the second cycle in $LiClO_4$ in DMF, FTIR spectra, ^{1}H solution NMR, and in situ DEMS of carbon electrode cycled in LiTFSI in DMF; FITR spectra, PXRD patterns, and ^{1}H NMR of electrodes discharged in DMA and NMP. This material is available free of charge via the Internet at http://pubs.acs.org.

AUTHOR INFORMATION

Corresponding Author

E-mail: p.g.bruce@st-andrews.ac.uk.

Notes

The authors declare no competing financial interest.

ACKNOWLEDGMENTS

P.G.B. is indebted to Toyota Motor Europe, to the EPSRC including the SUPERGEN program, and to ALISTORE, the European Network of Excellence on Lithium Batteries.

REFERENCES

(1) Abraham, K. M.; Jiang, Z. *J. Electrochem. Soc.* **1996**, *143*, 1.
(2) Read, J.; Mutolo, K.; Ervin, M.; Behl, W.; Wolfenstine, J.; Driedger, A.; Foster, D. *J. Electrochem. Soc.* **2003**, *150*, A1351.
(3) Ogasawara, T.; Debart, A.; Holzapfel, M.; Novak, P.; Bruce, P. G. *J. Am. Chem. Soc.* **2006**, *128*, 1390.
(4) Débart, A.; Paterson, A.; Bao, J.; Bruce, P. *Angew. Chem., Int. Ed.* **2008**, *47*, 4521.
(5) Kuboki, T.; Okuyama, T.; Ohsaki, T.; Takami, N. *J. Power Sources* **2005**, *146*, 766.
(6) Visco, S. J.; Katz, B. D.; Nimon, Y. S.; De Jonghe, L. C. PolyPlus Battery Company (Berkeley, CA) United States Patent, US20070117007, 2007.
(7) Imanishi, N.; Hasegawa, S.; Zhang, T.; Hirano, A.; Takeda, Y.; Yamamoto, O. *J. Power Sources* **2008**, *185*, 1392.
(8) Xu, W.; Xiao, J.; Wang, D.; Zhang, J.; Zhang, J.-G. *Electrochem. Solid-State Lett.* **2010**, *13*, A48.
(9) Hassoun, J.; Croce, F.; Armand, M.; Scrosati, B. *Angew. Chem., Int. Ed.* **2011**, *50*, 2999.
(10) McCloskey, B. D.; Scheffler, R.; Speidel, A.; Bethune, D. S.; Shelby, R. M.; Luntz, A. C. *J. Am. Chem. Soc.* **2011**, *133*, 18038.
(11) Beattie, S. D.; Manolescu, D. M.; Blair, S. L. *J. Electrochem. Soc.* **2009**, *156*, A44.
(12) Albertus, P.; Girishkumar, G.; McCloskey, B.; Sanchez-Carrera, R. S.; Kozinsky, B.; Christensen, J.; Luntz, A. C. *J. Electrochem. Soc.* **2011**, *158*, A343.
(13) Yang, X.-H.; He, P.; Xia, Y.-Y. *Electrochem. Commun.* **2009**, *11*, 1127.
(14) Laoire, C. O.; Mukerjee, S.; Abraham, K. M.; Plichta, E. J.; Hendrickson, M. A. *J. Phys. Chem. C* **2009**, *113*, 20127.
(15) Laoire, C. O.; Mukerjee, S.; Abraham, K. M.; Plichta, E. J.; Hendrickson, M. A. *J. Phys. Chem. C* **2010**, *114*, 9178.
(16) Lu, Y.-C.; Gasteiger, H. A.; Shao-Horn, Y. *J. Am. Chem. Soc.* **2011**, *133*, 19048.
(17) Mitchell, R. R.; Gallant, B. M.; Thompson, C. V.; Shao-Horn, Y. *Energy Environ. Sci.* **2011**, *4*, 2952.
(18) Peng, Z.; Freunberger, S. A.; Hardwick, L. J.; Chen, Y.; Giordani, V.; Bardé, F.; Novák, P.; Graham, D.; Tarascon, J.-M.; Bruce, P. G. *Angew. Chem., Int. Ed.* **2011**, *50*, 6351.
(19) Débart, A.; Bao, J.; Armstrong, G.; Bruce, P. G. *J. Power Sources* **2007**, *174*, 1177.
(20) Laoire, C. O.; Mukerjee, S.; Plichta, E. J.; Hendrickson, M. A.; Abraham, K. M. *J. Electrochem. Soc.* **2011**, *158*, A302.
(21) Wang, Y.; Zhou, H. *J. Power Sources* **2010**, *195*, 358.
(22) Hummelshoj, J. S.; Blomqvist, J.; Datta, S.; Vegge, T.; Rossmeisl, J.; Thygesen, K. S.; Luntz, A. C.; Jacobsen, K. W.; Norskov, J. K. *J. Chem. Phys.* **2010**, *132*, 071101.
(23) Wang, D.; Xiao, J.; Xu, W.; Zhang, J.-G. *J. Electrochem. Soc.* **2010**, *157*, A760.
(24) Zhang, G. Q.; Zheng, J. P.; Liang, R.; Zhang, C.; Wang, B.; Hendrickson, M.; Plichta, E. J. *J. Electrochem. Soc.* **2010**, *157*, A953.
(25) Black, R.; Oh, S. H.; Lee, J.-H.; Yim, T.; Adams, B.; Nazar, L. F. *J. Am. Chem. Soc.* **2012**, *134*, 2902.
(26) Wang, L.; Zhao, X.; Lu, Y. H.; Xu, M. W.; Zhang, D. W.; Ruoff, R. S.; Stevenson, K. J.; Goodenough, J. B. *J. Electrochem. Soc.* **2011**, *158*, A1379.

(27) Shimonishi, Y.; Zhang, T.; Imanishi, N.; Im, D.; Lee, D. J.; Hirano, A.; Takeda, Y.; Yamamoto, O.; Sammes, N. *J. Power Sources* **2011**, *196*, 5128.
(28) Bruce, P. G.; Freunberger, S. A.; Hardwick, L. J.; Tarascon, J.-M. *Nat. Mater.* **2012**, *11*, 19.
(29) Christensen, J.; Albertus, P.; Sanchez-Carrera, R. S.; Lohmann, T.; Kozinsky, B.; Liedtke, R.; Ahmed, J.; Kojic, A. *J. Electrochem. Soc.* **2012**, *159*, R1.
(30) Lee, J.-S.; Tai Kim, S.; Cao, R.; Choi, N.-S.; Liu, M.; Lee, K. T.; Cho, J. *Adv. Energy Mater.* **2011**, *1*, 34.
(31) McCloskey, B. D.; Bethune, D. S.; Shelby, R. M.; Girishkumar, G.; Luntz, A. C. *J. Phys. Chem. Lett.* **2011**, *2*, 1161.
(32) Freunberger, S. A.; Chen, Y.; Peng, Z.; Griffin, J. M.; Hardwick, L. J.; Bardé, F.; Novák, P.; Bruce, P. G. *J. Am. Chem. Soc.* **2011**, *133*, 8040.
(33) Freunberger, S. A.; Chen, Y. H.; Drewett, N. E.; Hardwick, L. J.; Barde, F.; Bruce, P. G. *Angew. Chem., Int. Ed.* **2011**, *50*, 8609.
(34) Sawyer, D. T.; Gibian, M. J.; Morrison, M. M.; Seo, E. T. *J. Am. Chem. Soc.* **1978**, *100*, 627.
(35) Sawyer, D. T.; Valentine, J. S. *Acc. Chem. Res.* **1981**, *14*, 393.
(36) Aurbach, D.; Zaban, A.; Schechter, A.; Ein-Eli, Y.; Zinigrad, E.; Markovsky, B. *J. Electrochem. Soc.* **1995**, *142*, 2873.
(37) Aurbach, D.; Daroux, M.; Faguy, P.; Yeager, E. *J. Electroanal. Chem.* **1991**, *297*, 225.
(38) Xu, W.; Viswanathan, V. V.; Wang, D.; Towne, S. A.; Xiao, J.; Nie, Z.; Hu, D.; Zhang, J.-G. *J. Power Sources* **2011**, *196*, 3894.
(39) Mizuno, F.; Nakanishi, S.; Kotani, Y.; Yokoishi, S.; Iba, H. *Electrochemistry* **2010**, *78*, 403.
(40) Bryantsev, V. S.; Blanco, M. *J. Phys. Chem. Lett.* **2011**, 379.
(41) Veith, G. M.; Dudney, N. J.; Howe, J.; Nanda, J. *J. Phys. Chem. C* **2011**, *115*, 14325.
(42) Wang, H.; Xie, K. *Electrochim. Acta* **2012**, *64*, 29.
(43) Assary, R. S.; Curtiss, L. A.; Redfern, P. C.; Zhang, Z. C.; Amine, K. *J. Phys. Chem. C* **2011**, *115*, 12216.
(44) Zhang, Z. C.; Lu, J.; Assary, R. S.; Du, P.; Wang, H. H.; Sun, Y. K.; Qin, Y.; Lau, K. C.; Greeley, J.; Redfern, P. C.; Iddir, H.; Curtiss, L. A.; Amine, K. *J. Phys. Chem. C* **2011**, *115*, 25535.
(45) Maricle, D. L.; Hodgson, W. G. *Anal. Chem.* **1965**, *37*, 1562.
(46) Peover, M. E.; White, B. S. *Electrochim. Acta* **1966**, *11*, 1061.
(47) Atkinson, R. *Int. J. Chem. Kinet.* **1997**, *29*, 99.
(48) Galliani, G.; Rindone, B. *Tetrahedron* **1981**, *37*, 2313.
(49) Curran, H. J.; Gaffuri, P.; Pitz, W. J.; Westbrook, C. K. *Combust. Flame* **1998**, *114*, 149.
(50) Matsumoto, S.; Sugimoto, H.; Sawyer, D. T. *Chem. Res. Toxicol.* **1988**, *1*, 19.
(51) Sinha, A.; Thomson, M. J. *Combust. Flame* **2004**, *136*, 548.
(52) Roberts, J. L.; Calderwood, T. S.; Sawyer, D. T. *J. Am. Chem. Soc.* **1984**, *106*, 4667.
(53) Wadhawan, J. D.; Welford, P. J.; Maisonhaute, E.; Climent, V.; Lawrence, N. S.; Compton, R. G.; McPeak, H. B.; Hahn, C. E. W. *J. Phys. Chem. B* **2001**, *105*, 10659.
(54) Ding, Y.; Kim, Y. J.; Erlebacher. *J. Adv. Mater.* **2004**, *16*, 1897.